Temporal Interaction of Tropical Cyclone Flood Drivers: A Multi-Scale Analysis from the North Atlantic Basin to Regional Watersheds

Ziyue Liu[a,c], Meredith L. Carr[b], Norberto C. Nadal-Caraballo[b], Michelle T. Bensi[a]
[a]Department of Civil and Environmental Engineering, University of Maryland, College Park, MD, USA. ziyue20@terpmail.umd.edu; mbensi@umd.edu
[b]Coastal & Hydraulics Laboratory, U.S. Army Engineer R&D Center, Vicksburg, MS, USA. meredith.l.carr@usace.army.mil; norberto.c.nadal-caraballo@usace.army.mil
[c]Edwardson School of Industrial Engineering, Purdue University, West Lafayette, IN, USA. liu4205@purdue.edu

Abstract: Tropical cyclone (TC)-induced coastal flooding can adversely affect critical infrastructure located along and near the coast. These flood events often result from multiple interacting flood drivers, including TC-induced storm surge, rainfall, river flooding, and wind. Mitigating the risks these hazards pose to critical infrastructure first requires assessing the frequency of compound flood events. In this study, we compile and analyze historical tidal and rainfall records across the U.S. Atlantic and Gulf coasts over an extended period. We identify limitations in existing long-term datasets, including incomplete temporal coverage and gaps in historical observations, and provide a systematic assessment of data availability to support future compound flood hazard analyses. We leverage the available data to conduct a multi-site correlation analysis to examine regional trends in the relationship between TC storm surge and rainfall across historical events. We also identify temporal offset patterns between surge and rainfall on a per-storm basis to better understand their interaction dynamics. We further undertake a local-scale analysis using higher-quality, more complete data in a selected subregion to investigate the correlation between flood driver intensity and temporal offset under different TC categories. This work improves the understanding of historical data availability and compound flood driver interactions in the U.S. Atlantic and Gulf coasts and provides a foundation for more robust compound flood hazard assessment and risk analysis.

1. INTRODUCTION

Tropical cyclone (TC)-induced coastal flooding causes substantial damage to critical infrastructure located along and near the coast. Such flooding can be compound in nature when multiple drivers, including storm surge, extreme rainfall, river discharge, and wind, interact to shape the overall hazard. Existing studies have developed a series of TC-induced coastal compound flood (CCF) probabilistic analysis frameworks that incorporate joint probability methods, machine learning, and Bayesian network methods [1-8].

Meanwhile, a growing body of research has focused on drivers' temporal interaction during CCF events. Because TC-induced CCF is fundamentally a complex temporal process, the sequencing and temporal offset between the peaks of individual drivers play a critical role in determining flood severity. Several studies have demonstrated strong relationships between inter-driver peak timing and resultant flood magnitude [9], [10, 11]. In addition, [12] analyzed compound flooding in New York City and found that TCs exhibit markedly different driver characteristics compared to other storm types. TCs dominate the joint probability of the most extreme rainfall-storm surge compound events, whereas extratropical cyclones are the primary drivers of more frequent, moderate compound events. In addition, [13] investigated the hydrometeorological and hydrological processes associated with Hurricane Florence using a combination of observational data and numerical simulations in the Cape Fear region of the U.S. They found that the shape of Florence's track induced much higher rainfall amounts than other

TCs, and therefore impacted the flood hydrograph at the basin scale. It provides further insight into the temporal mechanisms of TC-induced flooding.

In this study, we conduct a series of preliminary analyses at two spatial scales: separate large-scale analyses for the U.S. Atlantic and Gulf coasts, and a regional case study in the Cape Fear region for a more detailed investigation. This preliminary analysis is intended to provide an initial, data-driven characterization of the temporal interactions among TC-induced CCF drivers and to identify broad spatial and event-level patterns that can inform future, more detailed studies.

2. LARGE-SCALE ANALYSIS

We utilize the IBTrACS dataset [14, 15] and apply the historical storm data refinement procedure introduced by [16] to identify TC events impacting the U.S. Atlantic and Gulf coasts and extract the corresponding TC track time series for each event. We employ NOAA tide gauge data (https://api.tidesandcurrents.noaa.gov/api/prod/?) and NOAA rainfall observations (https://www.ncdc.noaa.gov/cdo-web/webservices/v2) to conduct a spatial analysis of the correlation between peak non-tidal residuals (NTR) during a TC event (hereafter referred to as TC peak NTR) and peak 24-hour moving-sum rainfall during a TC event (hereafter referred to as TC peak rainfall). In the large-scale analysis, we divide the study area into two coastal regions, the Gulf Coast and the Atlantic Coast, and conduct the correlation analysis separately for each region. Hourly NOAA rainfall data are used to compute TC peak rainfall. For tide gauge data, NTR is calculated by subtracting the predicted tidal component from the observed water level and are used to represent the portion of sea-level variability that primarily reflects storm surge effects [17]. For each NOAA tide gauge (observation site), the NOAA rainfall gauge closest in distance is selected to match it for later correlation analysis. The gauge locations are shown in Figure 1. Note that sites in Florida are included in both the Gulf Coast and Atlantic Coast regions in this analysis.

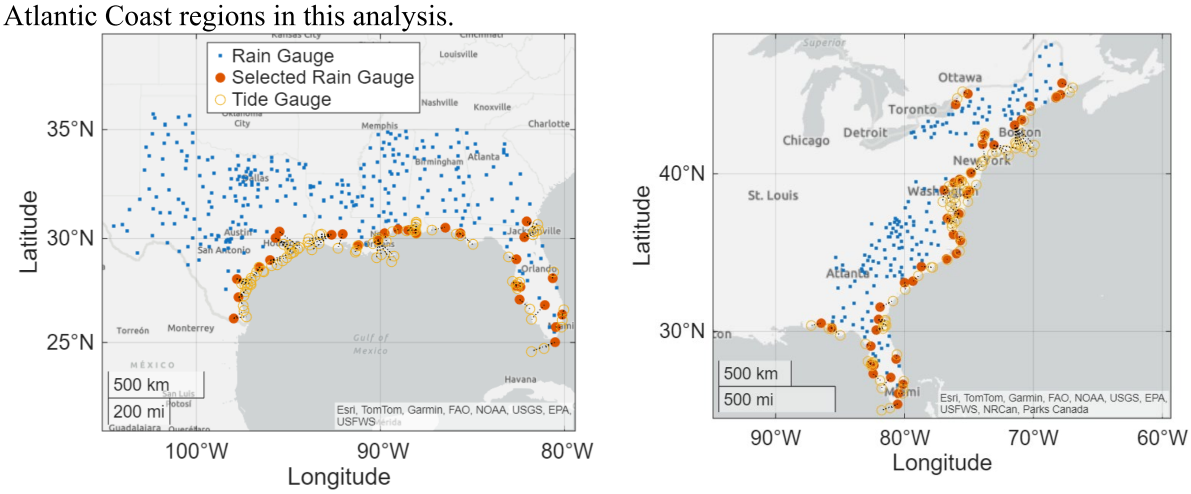

(a) **(b)**

Figure 1: Selected NOAA Rainfall and Tide Gauges. Paired rainfall and tide gauges are connected by dashed lines. (a) Gulf Coast; (b) Atlantic Coast

For each observation site, we obtain paired values of TC peak NTR and TC peak rainfall across historical TC events. We then calculate Kendall's τ correlation between these paired event-level peak values at each observation site. These site-specific correlations are then spatially interpolated using MATLAB's scatteredInterpolant function with the interpolation method set to "natural" and the extrapolation method set to "none". Figure 2 presents the resulting spatial patterns of the region-specific correlation analysis for the Gulf Coast and Atlantic Coast. Moderate to strong positive correlations between TC peak NTR and TC peak rainfall are observed across most areas, indicating compound hazard effects in both Gulf Coast and Atlantic Coast regions during TC events. We note that this spatial interpolation is used only to visualize broad spatial patterns in the site-specific correlation results, rather than to infer precise correlation values at ungauged locations. Because the availability and spatial density of NOAA tide and rainfall gauges vary substantially across the study region, the interpolated surfaces should be interpreted with caution, especially in areas with sparse observations.

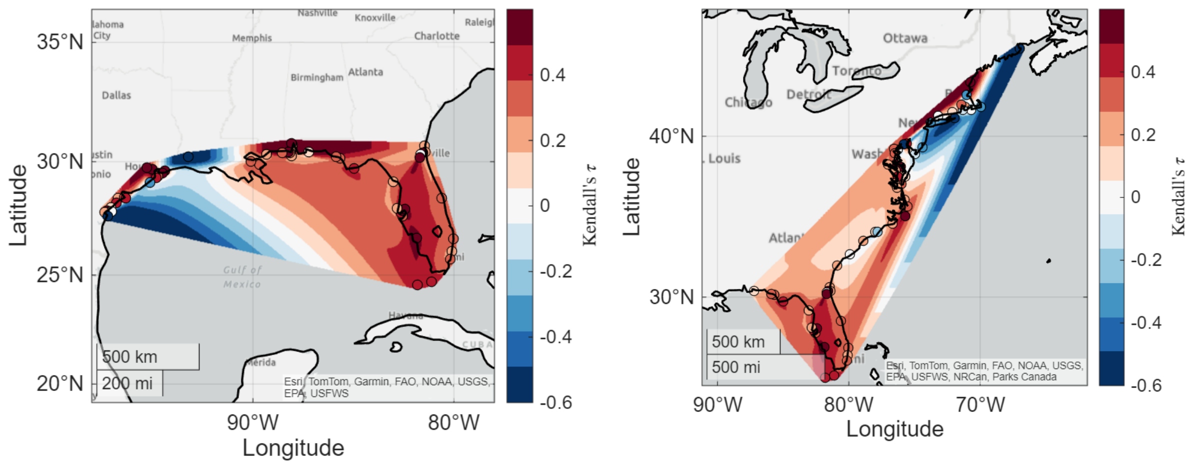

(a) **(b)**

Figure 2: Peak TC NTR-Rain Correlation Pattern; (a) Gulf Coast; (b) Atlantic Coast

To investigate the temporal interactions among CCF drivers (e.g., surge and rainfall), we conducted a peak event temporal offset analysis. We define the temporal offset as the number of hours by which TC peak NTR occurs before TC peak rainfall (a negative value indicates that the TC peak NTR occurs after the TC peak rainfall), and use this metric to investigate the temporal interactions among CCF drivers. Pairwise temporal offsets (in hours) between peak NTR and rainfall during TC events were computed for each TC event for each observation site pair. We begin with a statistical analysis of this temporal offset across all TC events. We evaluate whether the median temporal offset at each observation site pair is associated with its spatial location, using longitude for the Gulf Coast and latitude for the North Atlantic Coast. Figure 3 presents scatter plots of longitude versus median temporal offset for observation sites along the Gulf Coast, and latitude versus median temporal offset for observation sites along the North Atlantic Coast.

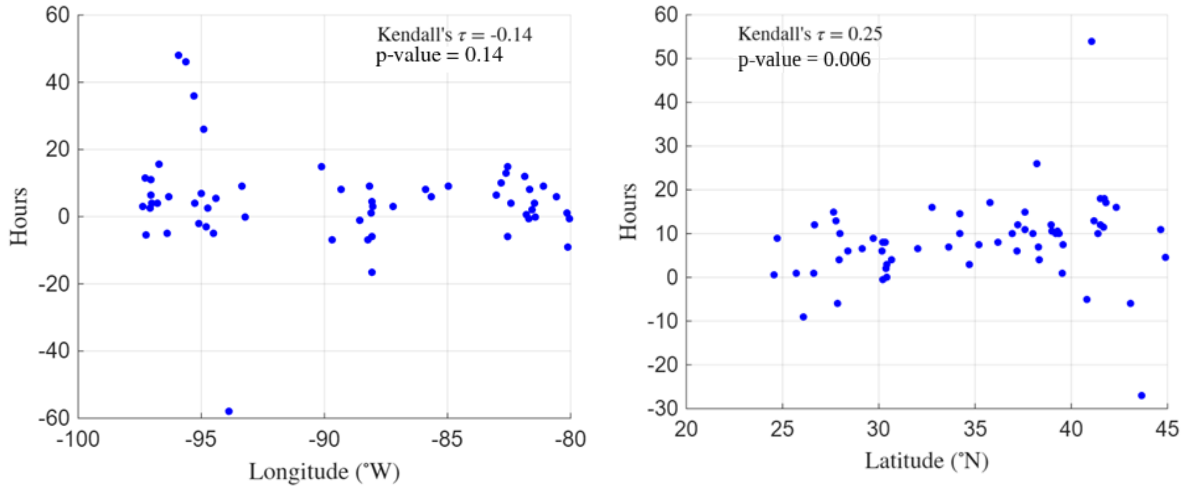

(a) **(b)**

Figure 3: Scatter Plots of Spatial Coordinates versus Median Temporal Offset. (a) Gulf Coast; (b) Atlantic Coast

The Gulf Coast results show a weak overall rank correlation between longitude and median temporal offset (τ = -0.14, p-value = 0.14), despite some visually apparent spatial patterns in the scatter plot. This weak overall correlation should be interpreted with caution because temporal offset values are missing for some site-event pairs due to variable NOAA tide and rainfall data availability across TC events and observation sites. In contrast, a moderate positive correlation is observed between latitude and median temporal offset along the North Atlantic Coast (τ = 0.25, p-value = 0.006). This suggests that along the

North Atlantic Coast, as latitude increases, TC peak rainfall is more likely to occur after the TC peak NTR.

Because this work presents a preliminary exploration, we use this analysis to identify broad spatial tendencies rather than to make definitive conclusions about coastwide temporal offset behavior. Future work will test the sensitivity of these results to event-selection criteria, missing-data thresholds, and alternative definitions of spatial location.

Although several studies have conducted temporal offset analysis in the U.S. Atlantic and Gulf coasts (e.g., [9, 12]), these analyses typically focus on the statistical properties of temporal offset across multiple storm events. In the next portion of this study, we investigated spatial temporal offset patterns on a per-storm basis within the North Atlantic basin. Specifically, we spatially interpolate temporal offset across the study region for each individual storm event, enabling visualization of spatial patterns of TC peak event temporal offset on a per-storm basis. We then subjectively select several storms as "master storms" and use the root mean square error metric to identify TCs with temporal offset patterns similar to those of the selected master storms.

The results reveal that, in the Gulf Coast region, temporal offset patterns exhibit greater variability with changes across TC events. In contrast, along the North Atlantic Coast, temporal offset patterns show less variability, particularly among TC events with similar TC tracks. Figure 4 presents examples of spatial temporal offset patterns with the corresponding TC tracks.

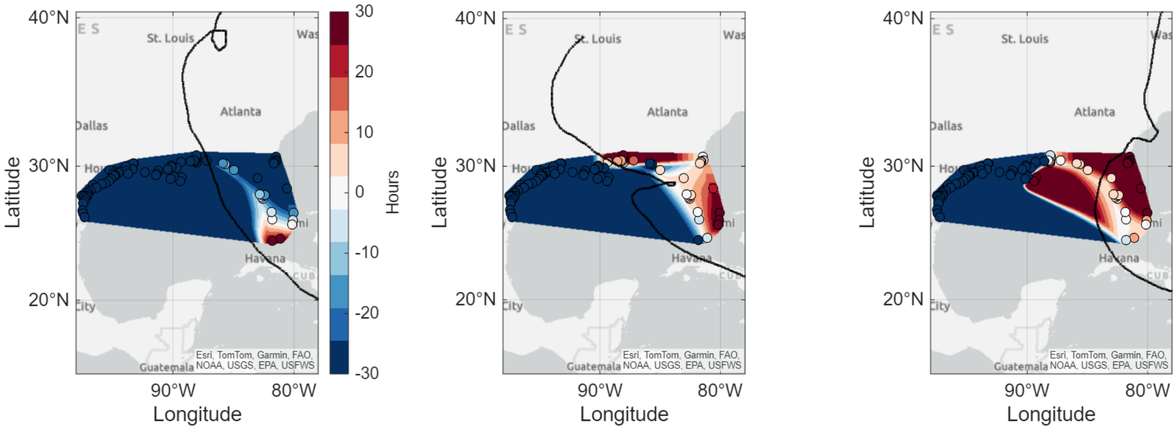

(a)

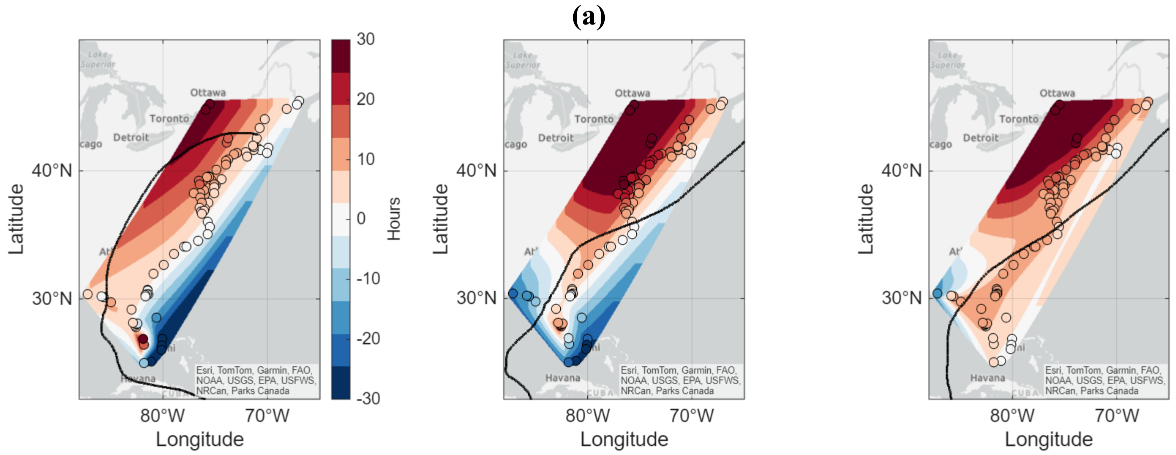

(b)

Figure 4: Examples of Spatial Temporal Offset Patterns with Corresponding TC Tracks. (a) Gulf Coast; (b) North Atlantic Coast

3. REGIONAL CASE STUDY IN CAPE FEAR

Building upon the large-scale data exploration, we selected the Cape Fear region for a regional analysis. This region was selected because previous studies have conducted CCF-related analyses in this area (e.g., [9, 13]), and because it has relatively well-established data availability and economic importance. Our case study analysis is conducted at six United States Geological Survey (USGS) gage sites across four Hydrologic Unit Codes (HUC) watershed basins. The relevant HUC basins and gauge locations are shown in Figure 5.

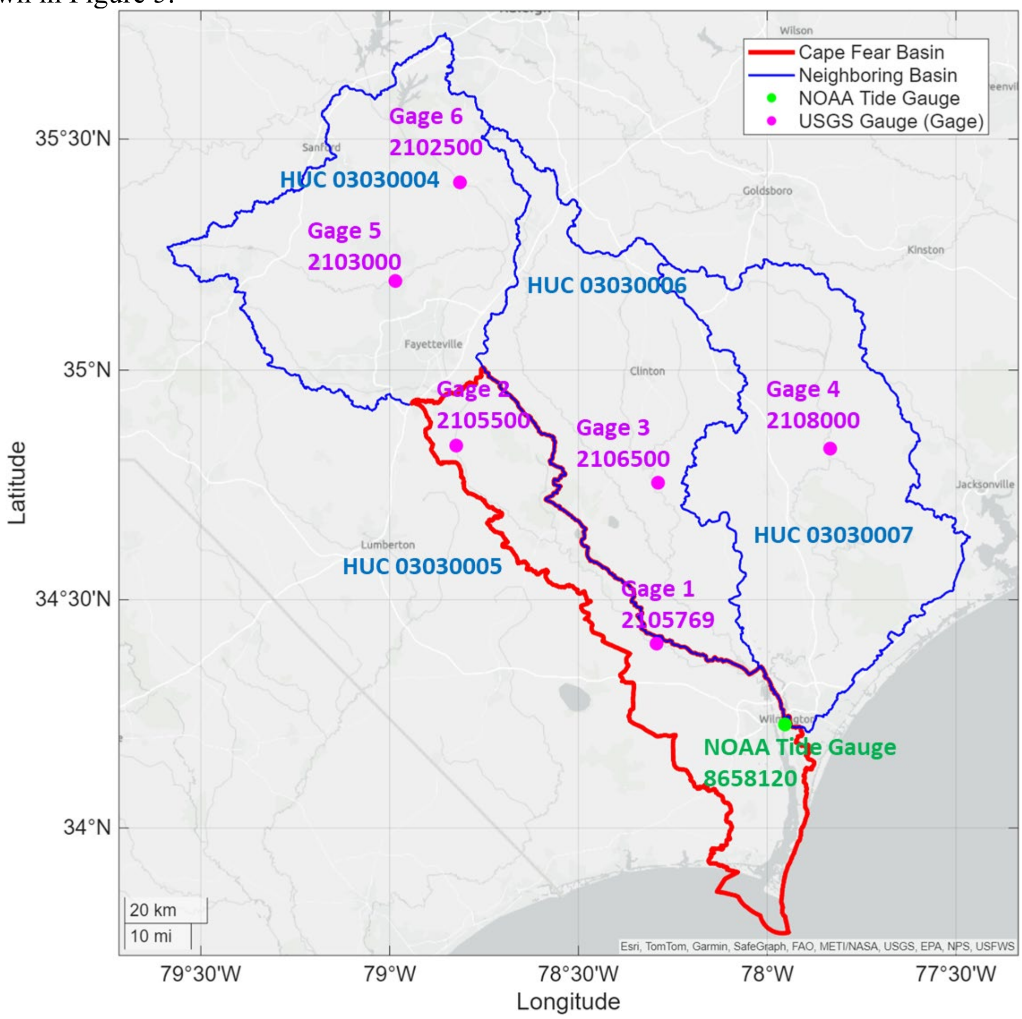

Figure 5: Map of the Regional Case Study and Gauge Locations. The rainfall data used in this analysis are extracted from AORC, no rainfall gauges are shown on the map

In this regional case study, we extract hourly rainfall data from the NOAA Analysis of Record for Calibration (AORC) database (https://registry.opendata.aws/noaa-nws-aorc/). For each HUC watershed basin, we compute the basin-averaged total rainfall time series using a moving 24-hour window. The NOAA tide gauge at Wilmington, NC (Station ID: 8658120) is selected because of its robust and continuous record from 1996 to the present, as well as its location downstream of the Cape Fear River.

Figure 6 shows examples of time series plots of NTR, rainfall, and gage height during a TC event using the extracted data. The figure illustrates the temporal co-occurrence and association among elevated NTR, rainfall, and gage height during the event.

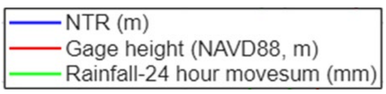

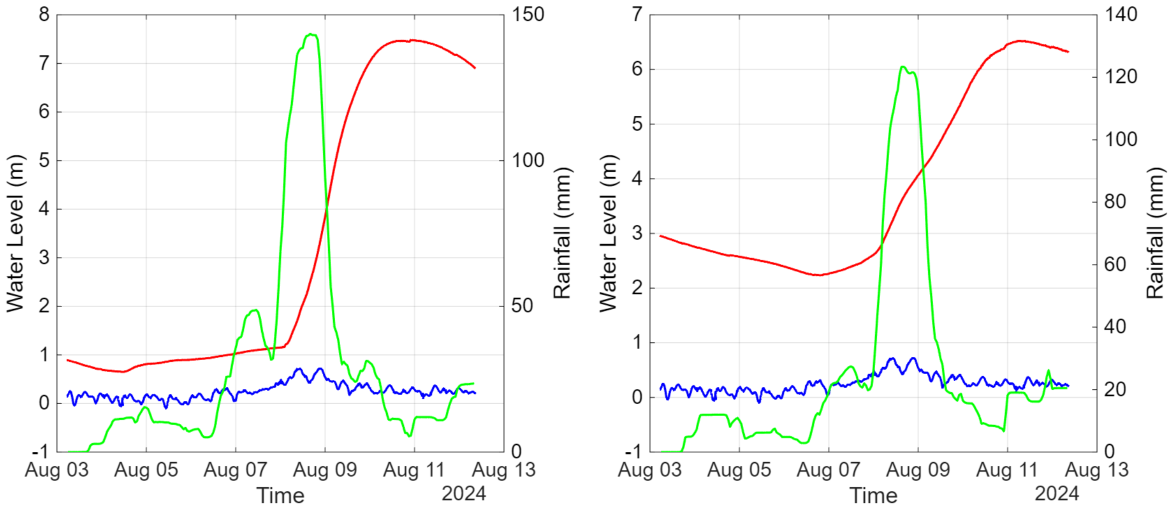

Figure 6: Examples of time series plots of NTR, rainfall, and gage height during a TC event. (a) Gage 1; (b) Gage 2

In the regional case study, we next extract the temporal offset between peak NTR and peak rainfall. Here, peak rainfall is defined as the maximum basin-averaged 24-hour moving-sum rainfall, which differs from the gauge-based TC peak rainfall used in the large-scale analysis. We then conduct a series of correlation analyses between the temporal offset and CCF driver intensity. Our results reveal a negative correlation between the absolute value of temporal offset and driver intensity in several cases. The absolute temporal offset is used because we found that positive and negative temporal offsets are approximately symmetrically distributed in a preliminary exploration.

Figure 7 presents scatter plots of TC peak rainfall and TC peak NTR versus absolute temporal offset, with color indicating TC intensity and the corresponding Kendall's τ values annotated. TC intensity is categorized based on the maximum central pressure deficit (CPD) of each event within a selected capture zone [18]: non-TC (NTC; CPD < 8 hPa), low intensity (LI; 8-28 hPa), moderate intensity (MI; 28-48 hPa), and high intensity (HI; 48-148 hPa). Overall, the results show that larger CCF driver magnitudes are generally associated with smaller absolute temporal offsets, suggesting stronger temporal alignment between peak rainfall and peak NTR during more intense events. The relationship between driver magnitude and absolute temporal offset varies by TC intensity class, with MI events exhibiting the strongest negative rank correlation. This pattern is mainly driven by the clustering of MI events near short temporal offsets, with a few lower-magnitude events occurring at longer temporal offsets. In contrast, LI storms show a wider spread in temporal offsets across a broad range of rainfall and NTR magnitudes, while HI storms tend to have larger rainfall and NTR values over a relatively narrower range of temporal offsets. These patterns suggest that temporal alignment between peak rainfall and peak NTR may be more consistent for moderate-intensity storms, whereas weaker storms exhibit greater variability in timing and high-intensity storms may be represented by fewer, more clustered events.

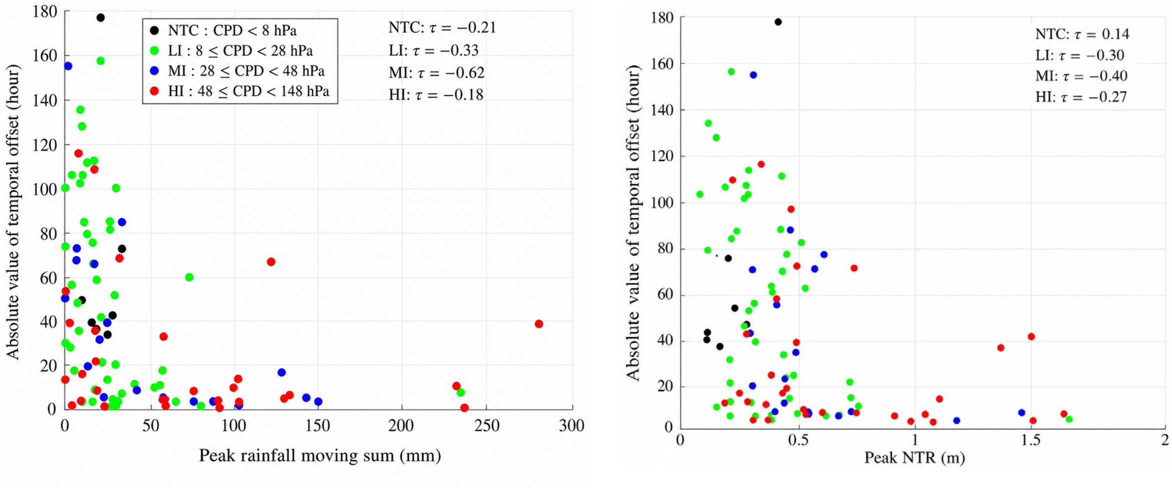

(a) Rainfall **(b) NTR**

Figure 7: Scatter plots of peak rainfall (a) and NTR (b) versus absolute temporal offset, color indicating TC intensity

Figure 8 presents scatter plots of TC peak rainfall and TC peak NTR versus absolute temporal offset, with color indicating storm forward velocity (V_f) and the corresponding Kendall's τ values annotated. Storm events are categorized based on the mean V_f within the selected capture zone: low (0-8 m/s), mid (8-15 m/s), and high (>15 m/s).

The results show that the largest peak rainfall and peak NTR values generally occur during low and mid V_f events, suggesting that slower-moving storms are associated with greater rainfall accumulation and coastal water-level response. However, the strongest negative correlation between peak rainfall and absolute temporal offset occurs for high V_f events, indicating that larger rainfall events within this class tend to have a smaller absolute temporal offset between rainfall and NTR peaks.

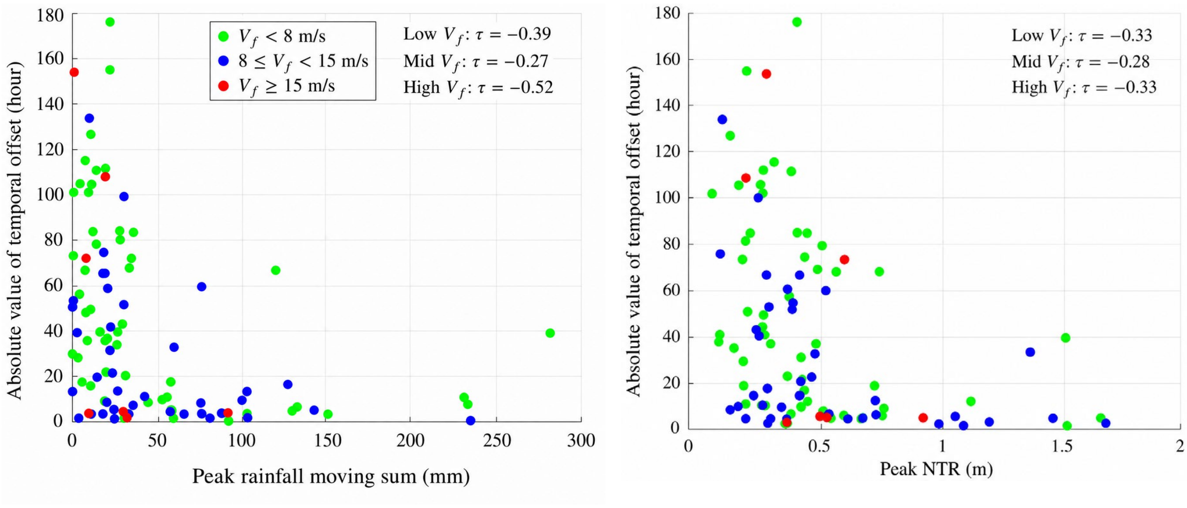

(a) Rainfall **(b) NTR**

Figure 8: Scatter plots of peak rainfall (a) and peak NTR (b) versus absolute temporal offset, color indicating event V_f

4. CONCLUSION

In this study, we compiled a comprehensive TC event dataset and conducted a series of analyses to investigate the temporal interactions among TC-induced CCF drivers along the U.S. Atlantic and Gulf coasts. These analyses are intended to provide an initial, data-driven characterization of how rainfall and coastal water-level processes are temporally related during TC events, and to serve as a building block for more detailed future studies of TC-induced compound coastal flooding. Our analysis spans two spatial scales.

At the large scale, we investigated both the U.S. Atlantic and Gulf coasts to evaluate the correlation between peak NTR and peak rainfall during TC events. The results show moderate to strong positive correlations across most regions, suggesting that compound hazard effects are prevalent along the U.S. Atlantic and Gulf coasts. We further analyzed the temporal offset between peak rainfall and peak NTR. When considering all TC events collectively, a significant positive relationship between temporal offset and latitude was identified along the North Atlantic Coast. At the individual storm level, the Gulf Coast exhibits more complex and variable temporal offset patterns, whereas the North Atlantic Coast shows relatively consistent temporal behavior, particularly for TCs with similar tracks.

Building on the large-scale analysis, we conducted a regional case study in the Cape Fear area. By integrating USGS gauge data, NOAA tide gauge data, and AORC rainfall data, we further investigated the relationship between temporal offset and TC-induced CCF drivers (e.g., rainfall and NTR) under different storm classifications. The results reveal that the relationship between driver magnitude and absolute temporal offset varies by TC intensity class, with moderate intensity TCs exhibiting the strongest negative rank correlation. Additionally, the most extreme rainfall and NTR values are generally associated with storms characterized by low to moderate storm forward speed V_f, suggesting that slower-moving storms may produce larger rainfall accumulation and surge response, while the temporal offset between rainfall and NTR peaks varies across events.

Acknowledgements

This study was supported by the USACE's Engineer Research and Development Center, Coastal and Hydraulics Laboratory (ERDC-CHL) under contract award number ID W912HZ25CA009. All opinions expressed in this paper are the authors' and do not necessarily reflect the policies and views of the research sponsor (USACE) or any other organization.

References

[1] N. C. Nadal-Caraballo, M. O. Campbell, V. M. Gonzalez, M. J. Torres, J. A. Melby, and A. A. Taflanidis, "Coastal Hazards System: A Probabilistic Coastal Hazard Analysis Framework," *Journal of Coastal Research*, vol. 95, no. sp1, p. 1211, May 2020, doi: 10.2112/SI95-235.1.

[2] S. Mohammadi *et al.*, "Bayesian-Motivated Probabilistic Model of Hurricane-Induced Multimechanism Flood Hazards," *Journal of Waterway, Port, Coastal, and Ocean Engineering*, vol. 149, no. 4, p. 04023007, Jul. 2023, doi: 10.1061/JWPED5.WWENG-1921.

[3] Z. Liu, M. L. Carr, N. C. Nadal-Caraballo, L. A. Aucoin, M. C. Yawn, and M. Bensi, "Comparative Analysis of Joint Distribution Models for Tropical Cyclone Atmospheric Parameters in Probabilistic Coastal Hazard Analysis," *Stochastic Environmental Research and Risk Assessment*, vol. 38, pp. 1741–1767, 2024, doi: https://doi.org/10.1007/s00477-023-02652-5.

[4] Z. Liu, M. L. Carr, N. C. Nadal-Caraballo, M. C. Yawn, and M. T. Bensi, "A Bayesian Network Method for Deaggregation: Identification of Tropical Cyclones Driving Coastal Hazards," May 20, 2025, *arXiv*: arXiv:2505.14374. doi: 10.48550/arXiv.2505.14374.

[5] Z. Liu, M. L. Carr, N. C. Nadal-Caraballo, L. A. Aucoin, M. C. Yawn, and M. T. Bensi, "A multi-tiered Bayesian network coastal compound flood analysis framework," *Coastal Engineering*, vol. 204, p. 104895, 2025, doi: 10.1016/j.coastaleng.2025.104895.

[6] Z. Liu, M. L. Carr, N. C. Nadal-Caraballo, M. C. Yawn, A. A. Taflanidis, and M. Bensi, "Machine Learning Motivated Data Imputation of Storm Data Used in Coastal Hazard Assessments," *Coastal Engineering*, vol. 190, 2024, doi: https://doi.org/10.1016/j.coastaleng.2024.104505.

[7] S. Agrawal, N. Hundia, Z. Liu, and M. Bensi, "Deep learning motivated data imputation of tropical cyclone radius of maximum winds," *14th International Conference on Structural Safety and Reliability - ICOSSAR'25*, vol. Applications of probability, statistics, and machine learning to the diverse field of Catastrophe Modeling, May 2025, doi: 10.23967/icossar.2025.065.

[8] Z. Liu, A. Al Kajbaf, and M. Bensi, "Applications of Statistical Learning Methods in Natural Hazard Assessment," presented at the Probabilistic Safety Assessment and Management & Asian Symposium on Risk Assessment and Management, Sendai, Japan, 2024. [Online]. Available: https://www.researchgate.net/profile/Ziyue-Liu-12/publication/387828835_Applications_of_Statistical_Learning_Methods_in_Natural_Hazard_Assessment/links/679a364a4c479b26c9c0c6cb/Applications-of-Statistical-Learning-Methods-in-Natural-Hazard-Assessment.pdf

[9] A. Gori, N. Lin, and D. Xi, "Tropical Cyclone Compound Flood Hazard Assessment: From Investigating Drivers to Quantifying Extreme Water Levels," *Earth's Future*, vol. 8, no. 12, p. e2020EF001660, 2020, doi: 10.1029/2020EF001660.

[10] H. Xu, X. Zhang, X. Guan, T. Wang, C. Ma, and D. Yan, "Amplification of Flood Risks by the Compound Effects of Precipitation and Storm Tides Under the Nonstationary Scenario in the Coastal City of Haikou, China," *Int J Disaster Risk Sci*, vol. 13, no. 4, pp. 602–620, Aug. 2022, doi: 10.1007/s13753-022-00429-y.

[11] H. Xu *et al.*, "Combining statistical and hydrodynamic models to assess compound flood hazards from rainfall and storm surge: a case study of Shanghai," *Hydrology and Earth System Sciences*, vol. 28, no. 16, pp. 3919–3930, Aug. 2024, doi: 10.5194/hess-28-3919-2024.

[12] Z. Chen *et al.*, "Influence of storm type on compound flood drivers of a mid-latitude coastal urban environment," *Hydrology and Earth System Sciences*, vol. 29, no. 14, pp. 3101–3117, Jul. 2025, doi: 10.5194/hess-29-3101-2025.

[13] D. Yin, Z. G. Xue, J. C. Warner, D. Bao, Y. Huang, and W. Yu, "Hydrometeorology and hydrology of flooding in Cape Fear River basin during Hurricane Florence in 2018," *Journal of Hydrology*, vol. 603, p. 127139, Dec. 2021, doi: 10.1016/j.jhydrol.2021.127139.

[14] J. L. Demuth, M. DeMaria, and J. A. Knaff, "Improvement of Advanced Microwave Sounding Unit Tropical Cyclone Intensity and Size Estimation Algorithms," *Journal of Applied Meteorology and Climatology*, vol. 45, no. 11, pp. 1573–1581, Nov. 2006, doi: 10.1175/JAM2429.1.

[15] NOAA, "International Best Track Archive for Climate Stewardship (IBTrACS)," National Centers for Environmental Information (NCEI). Accessed: Nov. 11, 2023. [Online]. Available: https://www.ncei.noaa.gov/products/international-best-track-archive

[16] Z. Liu and M. Bensi, "A Multi-Hazard Assessment Framework for Tropical Cyclones in South Korea: Data Development and Joint Probability Analysis," presented at the Probabilistic Safety Assessment and Management PSAM 18, Pittsburgh, Pennsylvania, 2026.

[17] D. Pugh, "Tides, Surges and Mean Sea-Level," in *Tides, Surges and Mean Sea-Level*, 1987. [Online]. Available: https://eprints.soton.ac.uk/19157/1/sea-level.pdf

[18] Nadal-caraballo, Norberto C *et al.*, “Coastal Hazards System - Louisiana (CHS-LA).” us army corps of engineers, Aug. 01, 2022. doi: 10.21079/11681/45286.